We are not the 99 percent: quantifying asphericity in the distribution of Local Group satellites

Jaime E. Forero-Romero [1] *, Verónica Arias[1]
[1] *Departamento de Física, Universidad de los Andes, Cra. 1 No. 18A-10 Edificio Ip, CP 111711, Bogotá, Colombia*

22 January 2018

ABSTRACT

We quantify the asphericity in the spatial distribution of the brightest satellites around the Milky Way (MW) and M31, the dominant galaxies in the Local Group (LG). We use simulations to build an explicit probability distribution for the asphericity around galaxies similar to the LG in the Lambda Cold Dark Matter paradigm. This allows us to estimate the atipicallity of the satellite distributions in the LG even when the underlying simulations do not have enough systems that fully resemble the LG. We demonstrate the method using three different simulations: Illustris-1, Illustris-1-DarkMatter and ELVIS. We find as a common trends in thse simulations that: i) at most of 1% the pairs are expected to have satellite distributions with the same degree of deviation from sphericity as the Local Group; ii) between 38% to 59% of the pairs have a halo with a satellite distribution as aspherical as in M31; and iii) at most 2% have a satellite distribution as planar as in the MW. These results place the LG close to the level of a 3-σ outlier in context provided by LCDM simulations.

Key words: Galaxies: halos — Galaxies: high-redshift — Galaxies: statistics — Dark Matter — Methods: numerical

1 INTRODUCTION

The presence of a Vast Polar Structure of satellites around the Milky Way has been stablished in the last decade. This structure can be easily described by global quantities of the brightest

The question whether this configuration is atypical in the observable universe cannot be proberly addressed given the current limits in observations. So far it has only been possible to contraint that 5% of the Milky-Way like galaxies in the Universe have two bright satellite galaxies as is the case of the Milky Way and its Large and Small Magellanic Clouds.

The closest system that could help us in providing a baseline for comparison is the Andromeda galaxy, M31. Its close enough that an observational study of its satellite population is possible, with the great advantage of having a perpective from a distance and not from within, as is the case for our Galaxy. These studies also found a planar satellite distributions. This time not in the whole distribution, but in a subset of 15 satellites out of an homogeneous sample of 27 satellites.

This has prompted a discussion on whether this satellite distributions are easily found in structure formation simu-

lations done in the current dominant paradigm for galaxy formation. This paradigm, based on a Cold Dark Matter cosmology in a expanding universe described by General Relativity with a Cosmological Constant, is the so-called Lambda Cold Dark Matter (LCDM).

The consensus is that these structures are hard to find in simulations. Some studies have focused on the study of individual dark matter halos that could host galaxies like the MW or M31, while some other studies have tried to simulate the formation of galaxy pairs resembling both the MW and M31. The transition from studying individual halos to pairs has been motivated by the hypotesis hat the location of the Local Group in the cosmic web should play a determinant role in building up planar satellite distributions through preferential alignments and accretions histories of galaxies.

Studies of the Local Group in an explicit cosmological context have also renewed the interest on performing constrained simulations that could reproduce the observed large scale structure of the Universe, This has also motivated the study of the two dominant galaxies in the Local Group as a pair in a cosmological context finding that the LG itself has relatively uncommon kinematic configuration in the context of LCDM and a strong preference to lie along filaments.

The aim of our work is to put together some of these pieces in a simple framework to quantify how atypical is the

---

* je.forero@uniandes.edu.co

satellite distribution found in the Local Group. Some of the explicit characteristics we want to keep in our treatment of the problem are the (i) cosmological context, (ii) the LG as a pair of galaxies and (iii) a simple and robust description for the satellites.

The first condition constrains the kind of simulations we use. We either results from fully cosmological simulations or resimulations of cosmological sub-volumes. The second condition constraints the kind of samples we want to use. We build explicit samples of pairs that resemble the kinematic structure of the MW and M31. The third condition motivates to only use the inertia tensor as a description for the satellites positions, while droping any information that might come from 3D velocities (high uncertainties) or involved algorithms for plane fitting.

Finally, to compute the odds of finding the LG satellite distributions in LCDM simulations, we do not make a direct search for the exact observed values into simulations because, as we show in Section, the LG is itself rare and we do not have enough simulated systems to perform such a brute force solution. We also avoid this direct comparison for a second reason. We do not want to implicitly use either LCDM or observations as what is considered normal or standard and compute the deviations from that point. Our approach is different. We set as a point of reference an spherical satellite distribution to quantify how both simulations and observations deviate from the spherical distribution. Simulations help us to construct an explicit probability distribution for deviations from sphericity in LCDM. Then we compute the odds of finding n satellite distributions that deviates from sphericity as much as the LG does.

In Section we list the sources of the observational and simulated data to be used throughout the paper. Next, in Section we describe the methods we use to quantify and characterize the satellite distributions. In section we present the results. In the discussion section we quantify the correlations between the main plane properties as described by the simulations. We use this results to quantify the degree of atipicality of the LG and estimate the volume that has to probed in simulations in order to find a pair with a satellite distribution as atipical as the LG. Finally, we summarize our conclusions in Section .

2 DATA SAMPLES

2.1 Observational Data

We use three dimentional positions as reported by. The appendix includes the tables with the values we use in our computations. For each central galaxy we use the 15 brightest satellites within a distance of 300kpc to the central galaxy. The satellites for the MW are: THe satellites for M31 are:

2.2 Data from the Illustris project

We use publicly available data from the Illustris Project (Vogelsberger et al. 2014). This suite of cosmological simulations, performed using the quasi-Lagrangian code AREPO (Springel 2010), followed the coupled evolution of dark matter and gas and includes parametrizations to account for the effects of gas cooling, photoionization, star formation, stellar

feedback, black hole and super massive black hole feedback. The simulation volume is a cubic box of 75 $\mathrm{Mpc}\,h^{-1}$ on a side. The cosmological parameters correspond to a ΛCDM cosmology consistent with WMAP-9 measurements (Hinshaw et al. 2013).

We extract halo and galaxy information from the Illustris-1 simulation which has the highest resolution in the current release of the Illustris Project. Illustris-1 has 1820^3 dark matter particles and 1820^3 initial gas volumen elements. This corresponds to a dark matter particle mass of $6.3 \times 10^6 \mathrm{M}_\odot$ and a minimum mass for the baryonic volume element of $8.0 \times 10^7 \mathrm{M}_\odot$. The corresponding spatial resolution is 1.4 kpc for the dark matter gravitational softening and 0.7 kpc for the typical size of the smallest gas cell size.

We buid a sample of Isolated Pairs that resemble the conditions in the LG. To construct this sample we select first all galaxies with an stellar mass in the range $1 \times 10^{10} \mathrm{M}_\odot < M_\star < 1.5 \times 10^{11} \mathrm{M}_\odot$. Then we consider the following criteria for all galaxies in that set.

• For each galaxy A we find its closest galaxy B, if galaxy A is also the closest to halo B, the two are considered as a pair.

• With d_{AB} the distance between the two galaxies and $M_{\star,min}$ the lowest stellar mass in the two galaxies, we discard pairs that have any other galaxy C with stellar mass $M_\star > M_{\star,min}$ closer than $3 \times d_{AB}$ from any of the pair's members.

• The distance d_{AB} is greater than 700 kpc.

• The relative radial velocity between the two galaxies, including the Hubble flow, is -120 km s$^{-1} < v_{AB,r} < 0$ km s^{-1}.

We find 27 pairs with these conditions. We then select the pairs where in both halos there are at least 15 detected subhalos, thus discarding pairs with halos with the lowest mass. We end up with a total of 20 pairs that fulfill these criteria, Appendix A shows the physical properties (stellar masses, maximum circular velocities, radial velocities and separation) in those pairs. This corresponds to a pair number density of 2×10^{-5} pairs Mpc^{-3}

Although Illustris-1 has stellar particles, we do not use their properties to select the satellite population because the smallest galaxies are barely resolved in stellar mass at magnitudes of $M_V = 9$. We prefer using the dark matter information as the smallest sub-halos are sampled with at least 35 particles. We chose the satellite samples by ranking the subhalos in decreasing order of its maximum circular velocity and select the first N_p halos in the list. The results presented here correspond to $11 \le N_p \le 15$.

2.3 Data from the ELVIS project

For a detailed description of the ELVIS project and data we refer the reader to. Here we summarize the elements relevant to our discussion. The data we use from the ELVIS project comes from the resimulation of dark matter halo pairs selected in dark matter only cosmological simulations. The parent cosmological boxes have a cosmology consistent with the Wilkinson Microwave Anisotropy Probe 7 results. They used the results from 50 simulation boxes of side lenght 70.4 Mpc to select pairs with kinematic characteristics similar to the LG. These selection criteria included the following

• The virial mass of each host must be in the range $1 \times 10^{12} M_\odot < M_{vir} < 3 \times 10^{12} M_\odot$

• The total pair mass must be in the range $2 \times 10^{12} M_\odot < M_{vir} < 5 \times 10^{12} M_\odot$

• The center of mass separation is in the range $0.6 \leq d \leq 1$ Mpc.

• The relative radial velocity is negative.

• No halos more massive than the least massive halo within 2.8 Mpc and no halos with $M_{vir} > 7 \times 10^{13}$ within 7 Mpc of the pairs' center of mass.

This corresponds to a pair number density of 8×10^{-6} pairs Mpc^{-3}, this is a factor 2.4 lower than the pair number density we find in Illustris-1. There were a total of 146 pairs that met those criteria, but only 12 were chosen for resimulation. Additionally, the selected pairs for resimulation have a relative tangential velocity less than 75 km s^{-1}. In this paper we only use the results from the 12 resimulated pairs.

3 BUILDING, CHARACTERIZING AND COMPARING SATELLITES SPATIAL DISTRIBUTIONS

3.1 Building Satellite Samples

We compare the joint satellite distributions in the MW and M31 at fixed satellite number, N_s. This means that the magnitude cut corresponding to the faintest satellite included in the sample is different in each case. We make this choice for two reasons. First, to be sure that there is a non-zero number of satellites in the simulations to make the computations. Second, to rule out the influence of satellite numbers in the statistics.

We compute the satellite statistics fo 11 up to 15 satellites. The lowest bound corresponds to the number of classical Milky Way satellites. The upper limit corresponds to the maximum number of satellites that can be resolved in both halos for most of the isolated pairs in Illustris-1. In simulations we rank the subhalos by their maximum circular velocity, in observations we rank the satellites by its M_V magnitude.

We also use two kinds of satellite distributions. The first keeps the positions for the satellites fixed as provided in the observations/simulations; the second randomizes the angular positions of the satellites around the central galaxy while keeping its radial distance fixed. The randomization process is done 1000 times for each galaxy.

3.2 Describing Samples with the Inertia Tensor

We base all our results on the description provided by the inertia tensor defined by the satellites's positions.

$$\bar{\mathbf{I}} = \sum_{k=1}^{N_s} [(\mathbf{r_i} - \mathbf{r_0})^2 \cdot \mathbf{1} - (\mathbf{r_i} - \mathbf{r_0}) \cdot (\mathbf{r_i} - \mathbf{r_0})^{\mathbf{T}}], \qquad (1)$$

where k indexes the set of satellites of interest $\mathbf{r_k}$ are the satellites' positions, $\mathbf{r_0}$ is the location of the central galaxy $\mathbf{1}$ is the unit matrix, and $\mathbf{r}^T$ is the transposed vector $\mathbf{r}$. We use $\mathbf{r_0}$ as the position of the central galaxy, and not the satellites' geometrical center, to allow for a fair comparison

once the angular positions of the satellites are randomized around this point.

From this tensor we compute its eigenvalues, $\lambda_1 > \lambda_2 > \lambda_3$, and corresponding eigenvectors, $\hat{I}_1, \hat{I}_2, \hat{I}_3$. We define the size of the three ellipsoidal axis as $a = \lambda_1$, $b = \lambda_2$ and $c = \lambda_3$. We also define $\hat{n} \equiv \hat{I}_1$ as the vector perpendicular to the planar satellite distribution. We also define the width, w, of the planar satellite distribution, as the standard deviation of all satellite distances to the plane defined by the vector $\hat{n}$.

To summarize we characterize the satellite distribution by for quantities obtained from the inertia tensor:

• Plane width, w.
• c/a axis ratio.
• b/a axis ratio.

3.3 Comparing Satellite Samples

We compare every satellite distribution against its own spherically randomized distribution. We keep fixed the radial position of every satellite with respect to the central galaxy and then randomizing its angular position. We repeat this procedure 1000 times for each satellite distribution and proceed to measure the quantities mentioned in the last section: w, c/a and b/a. For each quantity we compute an average and standard deviation from the 1000 random samples. This allows us to build a normalized version of all quantities of interest by substracting the mean and dividing between the standard deviation of the randomized samples.

This allows us to make a first comparison. The observed/simulated distribution against its randomized version. The second intermediate comparison we make are observations against simulations. The final comparison is between the normalized quantities, both observed and simulated.

The comparison between the normalized quantities is the one that carries the important information about the deviations from sphericity. We do not want to directly compare how the results observations deviate from simulations but to compare the deviations from asphericity in observations and simulations.

3.4 Describing joint satellite distributions

After building the normalized variables with the simulated data we perform a Kolmogorov-Smirnov test with the null hypothesis of belongig to a normal distribution with mean and standard deviation computed from the mean and standard deviation from the data itself. We find that the distributions for w, c/a and b/a cannot reject the null hypothesis.

We then build a multivariate normal distribution for the two halos and the three variables consistent with a unidimensional normal distribution using the vector of mean values and covariance matrix. This means that our final covariance matrix is 6×6 and takes into account the correlations internal to a single galaxy and with its partner. We compute the preferred covariance matrix and the mean distribution values with a jackknife technique. That is, out of the the n pairs we have, we perfom n different covariance and mean value measurement using only $n - 1$ pairs. The

reported covariance and mean values correspond to the average of all measurements, the corresponding standard deviation also help us to estimate the uncertainty on every reported coefficient.

This compact description allows us to generate samples of size N that are consistent by construction with their parent simulation. Finally, we use the generated samples to estimate how commoon are the deviations from sphericity that we measure in the observational data. We use a single-tail test in this comparison, meaning that we always measure the fraction of points with values smaller than the treshold value.

4 RESULTS

4.1 Plane Width

Figure 1 summarizes the results for the plane width distributions. The panel on the left compares the results for the MW and M31 observations against its randomized version. The most interesting outcome is that the MW plane width is smaller than $\approx 98\%$ of the planes computed from the randomized distribution, while the M31 plane width is consistent with the same distribution.

4.2 c/a axis ratio

Figure 2 shows the results for the minor to major axis ratio. Corresponding in the ELVIS data are in the appendix in Figure B1.

The left panel shows the results for the LG compared against its spherically randomized version. As expected the c/a ratio in the MW is significantly lower as the measured values for spherical distributions. On the other hand the ratio for M31 is lower than the mean of the spherical values but still well within its variance. In contrast to the results for the plane width, this time the randomized values have symmetrical expectations between the two galaxies.

The middle panel shows the LG compared against the results from Illustris. In this case we find a similar trend. The MW is atypical and M31 is within the variance from the simulation data. This time, however, there is a single MW-like galaxy out of the total of 20 that shows an c/a as small as the MW. The only assymetry evident between the simulated halos is in the dispersion, the c/a distribution for the massive halos seems to be wider than it is for the less massive partner.

The right panel shows the normalized results. This highlights the two results mentioned above. First, the MW shows a low c/a ration close to two standard deviations away from the mean value of the spherical distribution; this contrasts the results for M31 which are close to 1 standard deviation away. Second, the less massive halos in the Illustris simulation present a smaller dispersion in their deviations from sphericity than the its masssive partner. The MW axis ratio smaller than $\approx 98\%$ of the randomized satellite distributions. and its atipicallity is only comparable to one halo in the Illustris simulation (none in the ELVIS simulation).

4.3 b/a axis ratio

Figure 3 shows the results for the minor to major axis ratio. Corresponding in the ELVIS data are in the appendix in Figure B1. In all cases of comparison (against randomized distribution, comparasion against simulations and degree of deviation from sphericity) the results for both the MW and M31 do not seem atypical or deviated from the expectations for an spherical dsitribution.

4.4 Multivariate Distributions

This is all the information that is needed to compute the fraction of pairs that are expected to share the same asphericity as the LG. We start the Discussion section by describing the results of performing such a computation.

5 DISCUSSION

6 CONCLUSIONS

In this paper we develop and demostrate a method to quantify the asphericity of the satellite distribution in the Local Group. The method uses as a basic condition the spherical randomization of satellite positions (observed or simulated). The scalars describing the satellite distribution in each galaxy are then normalized to the mean value and standard deviation in the randomized samples. In observations we limit our analysis to the 11 brightest satellites in the Milky Way and Andromeda. For numerical data we use the Illustris-1 and the ELVIS simulations.

We find that the deviation from aesphericity in the LG is only expected in 1 ± 3 pairs out of a sample of 2000 isolated pairs. This places the LG as a 3σ outlier. The weight to explain this atypical result is not distributed equally between the MW and M31. While M31 presents a fully typical asphericity in the expectations from LCDM, the MW shows aspherical deviations in plane width and the major-to-minor axis ratio highly atypical in the framework of LCDM. We estimate that with the M31 XX out of 2000 pairs show normalized characteristics larget r equal than M31, while this number drops to XX for the MW.

The method we present to quantify how atypical is the LG is robust to the numerical simulations used to define the LCDM expectations. Quantifying the degree of asphericity highlights the atypicality of the Milky Way stressing the stark difference with M31 and its more typical nature. This atypical distribution also adds up to the presence of two bright satellite galaxies, which is also uncommon both in simulations and observations.

The extension of the framework we present in this paper to describe outliers found as a second order deviation (i.e. fiding a *subset* of satellites in M31 that are in a plane or *adding* velocity information) could also be possible along the line of work presented by, that avoid finding in observations the exact observed distribution and instead focuse in defining atypicallity.

The quantitative study we present allows us to estimate the volumes that cosmological simulations have to probe in order to study similar LG configurations. Such atypical satellite distribution should be seen as an opportunity to
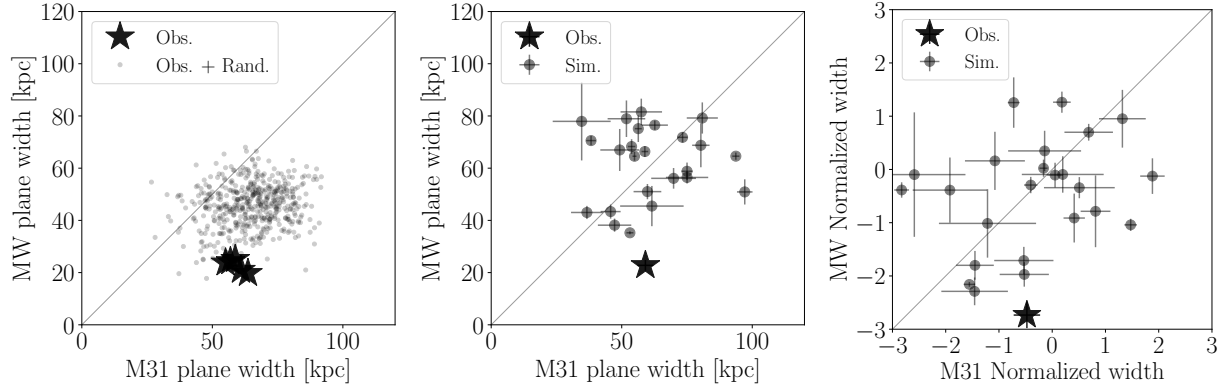
Figure 1. Plane width characterization in the Local Group and the Isolated Pairs. In all panels the horizontal axis corresponds to the M31 or the most massive halo in the pair and the vertical axis to the MW or the least massive halo in the pair. The panel on the left shows the plane width in physical units comparing the results from observations (stars) against the result of spherically randomizing the satellite positions while keeping its radial distance (circles). The panel in the middle compares the average from the observations (star) and the average from each one of the Isolated Pairs (circles with error bars). The panel on the right has the same information as the middle panel, only that this time each point has been normalized (median substracted and normalized by the standar deviation) to the results of its randomization. The main message of this series of plots is that the MW has a significantly thiner plane both compared to the result of its own satellite spherical randomization (left panel) and the expectation from simulations (middle panel). This low value is 2σ away from what is expected in a spherical distribution. In the M31 their satellites are in agreement with the expectations both from an spherical distribution and the results form the simulations. A second conclusion is that the spherically averaged plane width MW (seen in the point cloud in the left panel) is smaller than the average expectation from simulations, while for M31 the spherical average is consistent with simulations.
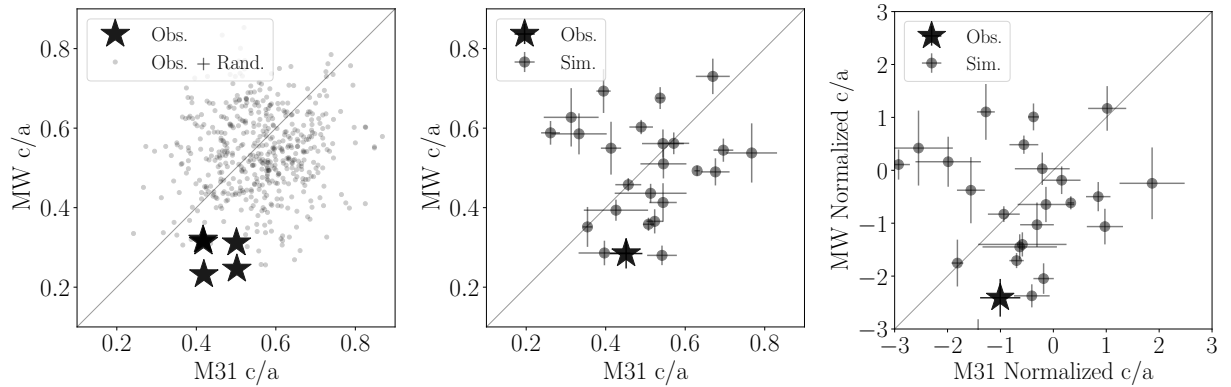

Figure 2. Same layout as in Figure 1. This time for the c/a axis ratio. The message holds in this case as for the plane width. The MW is has a significantly low c/a value compared to the expectation from a spherical distribution and simulations. This low value is also 2σ away from the expactations for an spherical distribution. M31 is consistent both with an spherical distribution and the results from simulations. However, in this case the axis ratio in the spherically averaged case is completeley consistent with the expectation from simulations.

	Observations		Randomized Obs.		Illustris-1		ELVIS	
	M31	**MW**	**M31**	**MW**	**M31**	**MW**	**M31**	**MW**
Plane width (kpc)	59 ± 3	22 ± 2	64 ± 12	45 ± 8	70 ± 4	67 ± 2	70 ± 2	68 ± 4
c/a ratio	0.45 ± 0.04	0.28 ± 0.03	0.55 ± 0.10	0.53 ± 0.10	0.52 ± 0.01	0.53 ± 0.01	0.54 ± 0.01	0.49 ± 0.02
b/a ratio	0.82 ± 0.06	0.78 ± 0.02	0.82 ± 0.07	0.81 ± 0.08	0.80 ± 0.01	0.80 ± 0.02	0.80 ± 0.01	0.81 ± 0.01

Table 1. Mean values and standard deviations for the different quantities describing satellite distributions: plane width, c/a ratio and b/a ratio. The first colum refers to the results from observational data, the second column uses the spherically randomized version of the observational data. The third column summarizes the results from the 20 pairs in Illustris-1 and the last column corresponds to the 12 pairs in the ELVIS project.
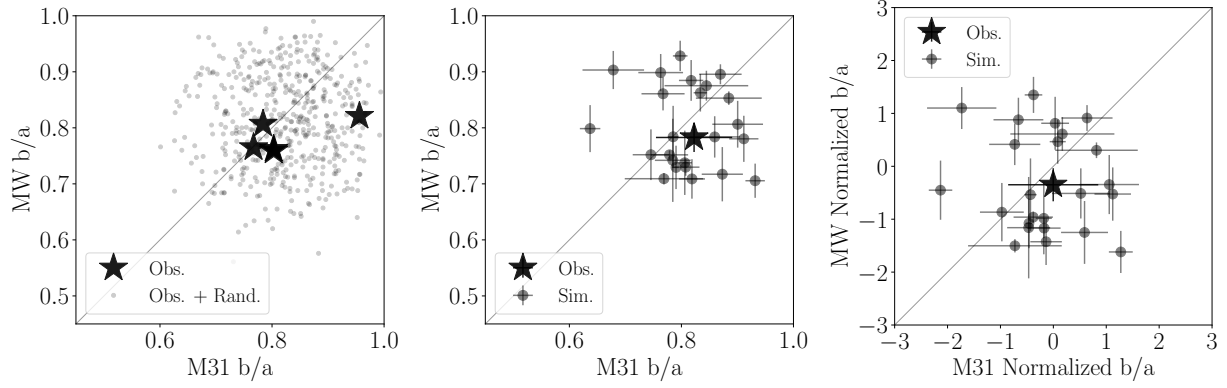
Figure 3. Same layout as in Figure 1. This time for the b/a axis ratio. In this case both the MW and M31 are consistent with the results of a spherical distribution and the simulations.
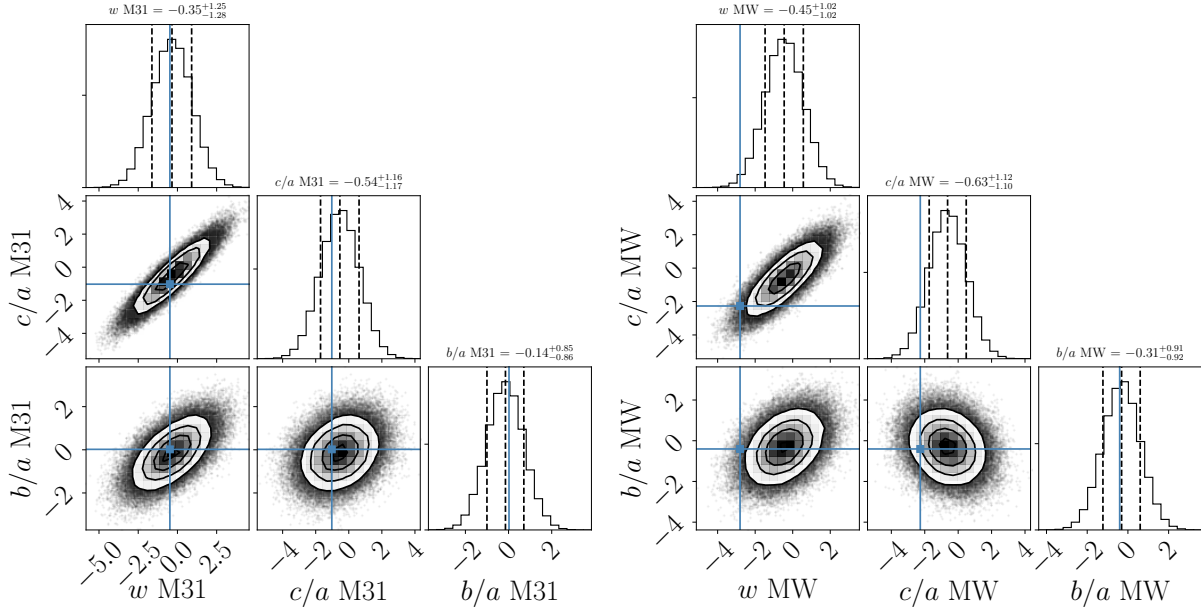

Figure 4. Correlations between the multivariate gaussian model built on the normalized values for the plane width w, c/a ratio and b/a ratio. Left/right panel correspond to M31/MW. The contour levels in the 2D histograms correspond to the 1σ, 2σ and 3σ contours in two dimensions. The dahsed vertical lines in the histograms along the diagonal correspond to the 1σ boundaries in one dimension. The results for the gaussian model are built from 10^6 point realizations in the six-dimensional space spaned by the variables of interest. The correlation matrix and the mean values are computed from the results in the Illustris-1 simulation. The cross indicates the LG values. This plot clearly shows how the M31 results are well within the expectations from simulations while MW has an unusual low value for the plane width and the c/a axis ratio. Equivalent results from the ELVIS data are presented in Figure B2.

constraint in high detail the initial conditions and environment that allowed such pattern to emerge.

REFERENCES

Hinshaw G., et al., 2013, ApJS, 208, 19
Springel V., 2010, MNRAS, 401, 791
Vogelsberger M., et al., 2014, MNRAS, 444, 1518

APPENDIX A: PHYSICAL CHARACTERISTICS OF THE ISOLATED PAIRS SAMPLES

APPENDIX B: RESULTS FROM ELVIS

APPENDIX C: COVARIANCE MATRICES AND MEAN VALUE VECTORS

Illustris M31
    Covariance

```
[[ 0.83+/-0.03  0.78+/-0.04  0.41+/-0.04]
 [ 0.78+/-0.04  1.16+/-0.05 -0.15+/-0.05]
 [ 0.41+/-0.04 -0.15+/-0.05  0.96+/-0.04]]
```
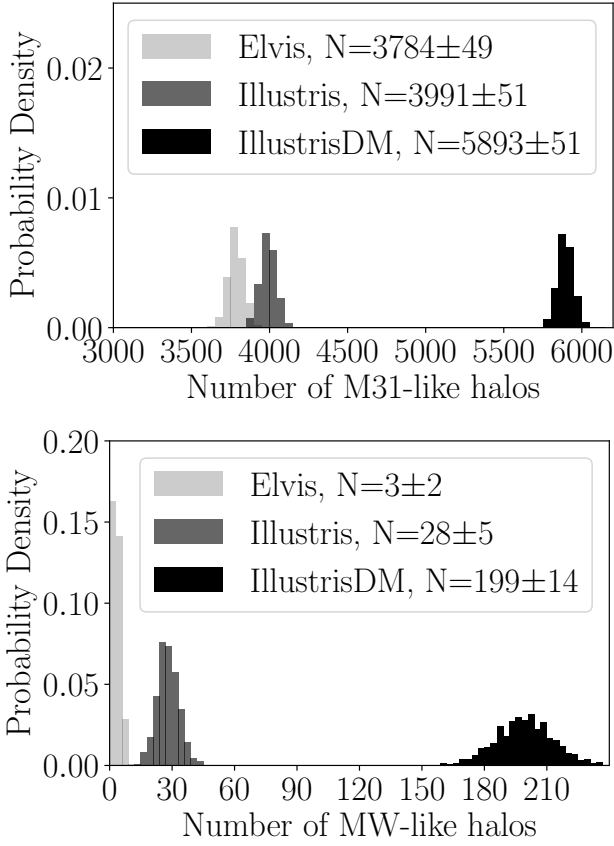
Figure 5. Probability distribution for the expected number of M31 and MW halos showing the same degree of atipicality as the Local Group if drawn from a sample of 10000 isolated pairs. The distributions correspond to results derived from Illustris-DM, Illustris, and ELVIS data. In the most optimistic case (Illustris-DM), 1% of the pairs have two halos with properties similar to the LG. In the case of Illustris this percentage drops to 0.1% and 0.01% for ELVIS.

Mean

[-0.18+/-0.04 -0.41+/-0.05 -0.20+/-0.05]

Illustris MW

[[0.78+/-0.06 0.63+/-0.07 0.40+/-0.03]
 [0.63+/-0.07 0.69+/-0.08   0.06+/-0.02]
 [0.40+/-0.03 0.06+/-0.02   0.61+/-0.04]]

Mean

[-0.17+/-0.04 -0.40+/-0.04 -0.23+/-0.04]

IllustrisDM M31
Covariance

[[1.50+/-0.08 1.27+/-0.08 0.64+/-0.04]
 [1.27+/-0.08 1.31+/-0.08 0.28+/-0.04]
 [0.64+/-0.04 0.28+/-0.04 0.70+/-0.04]]

Mean

[-0.37+/-0.05 -0.55+/-0.05 -0.13+/-0.03]

IllustrisDM M31
Covariance

[[1.03+/-0.05   0.94+/-0.05   0.36+/-0.03]
 [0.94+/-0.05   1.24+/-0.07 -0.18+/-0.04]
 [0.36+/-0.03   -0.18+/-0.04 0.86+/0.03]]

Mean

[-0.45+/-0.04 -0.61+/-0.05 -0.31+/-0.04]

ELVIS M31
Covariance

[[1.60+/-0.19 1.22+/-0.14 0.70+/-0.09]
 [1.22+/-0.14 1.08+/-0.10 0.35+/-0.05]
 [0.70+/-0.09 0.35+/-0.05 0.63+/-0.10]]

Mean

[-0.18+/-0.08 -0.28+/-0.07 -0.22+/-0.05]

ELVIS MW Covariance

[[0.45+/-0.04   0.61+/-0.09 -0.11+/-0.09]
 [0.61+/-0.09   1.21+/-0.17 -0.63+/-0.09]
 [-0.11+/-0.05   -0.63+/-0.09 0.64+/-0.06]]

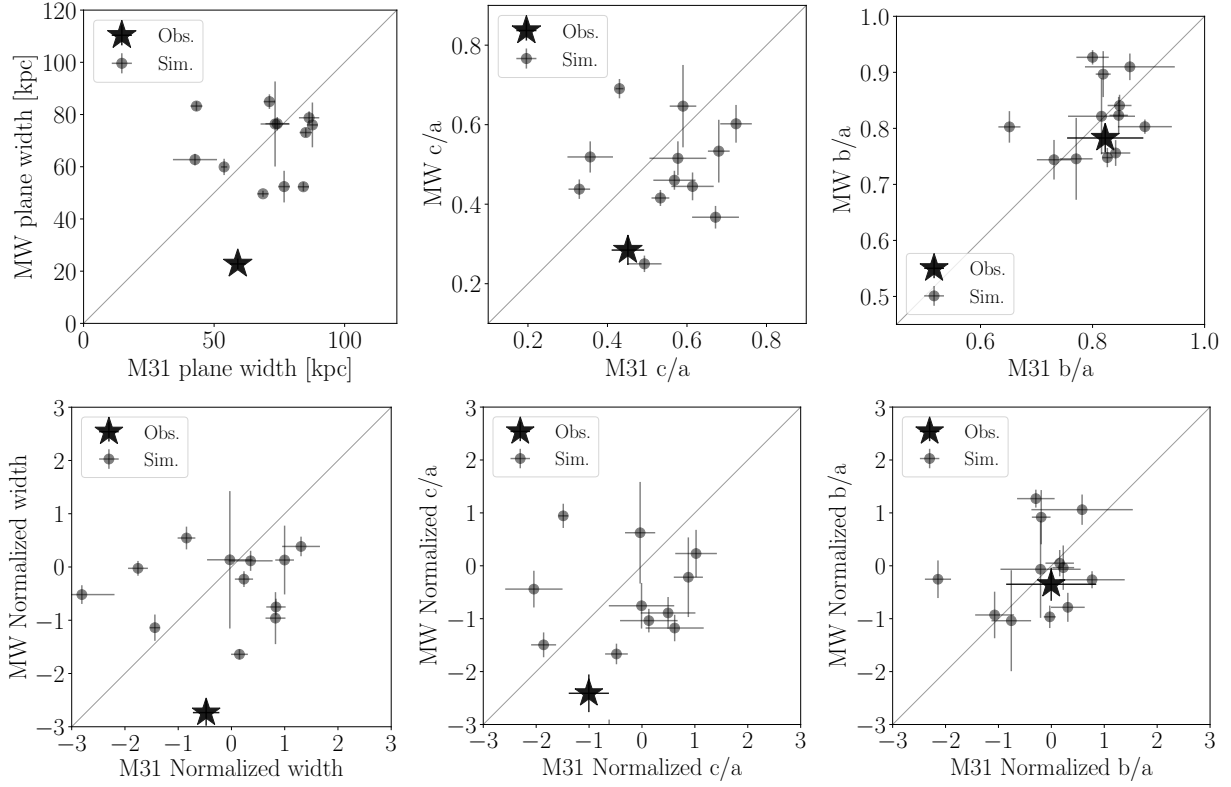[-0.32+/-0.04 -0.74+/-0.07 -0.08+/-0.05]

Figure B1. ELVIs results for the quantities presented for the Illustris-1 simulation in Figures 1, 2, 3. Upper row corresponds to the raw values from observations and simulated pairs, while the second row normalizes the same values to the mean and standard deviation on its spherically randomized counterparts.
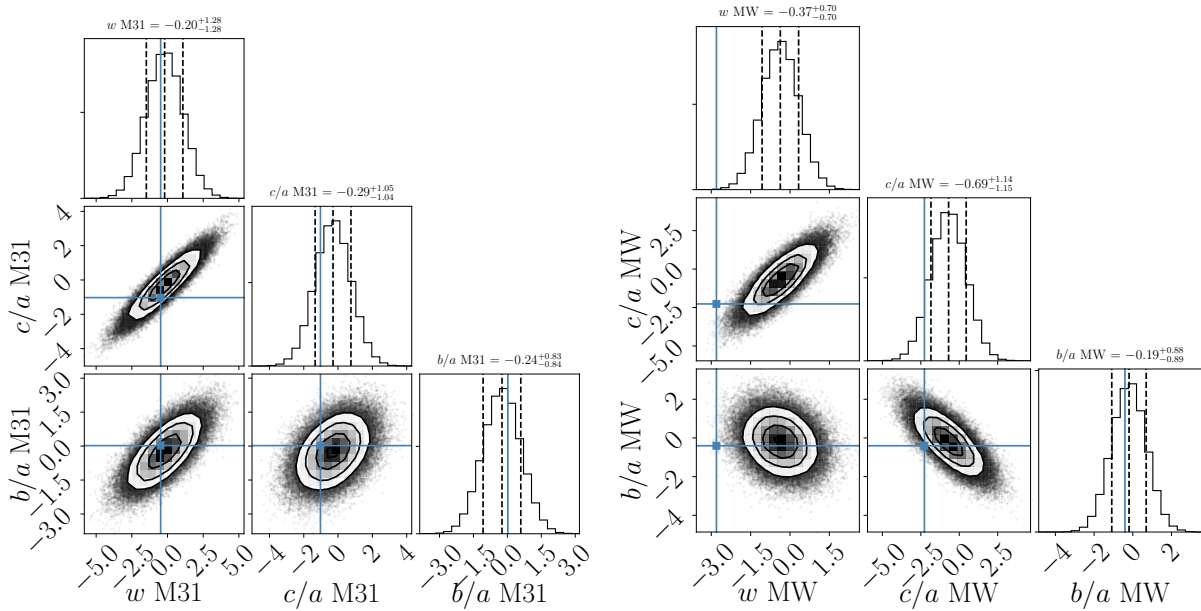

Figure B2. Same layout as Figure 4, this time computed from the ELVIS data.